

www.acsanm.org Forum Article

Quantitative Energy Transfer in Organic Nanoparticles Based on Small-Molecule Ionic Isolation Lattices for UV Light Harvesting

Junsheng Chen, ¹ Stine G. Stenspil, ¹ Spyridon Kaziannis, Laura Kacenauskaite, Nils Lenngren, Miroslav Kloz, Amar H. Flood, * and Bo W. Laursen *



Cite This: ACS Appl. Nano Mater. 2022, 5, 13887-13893



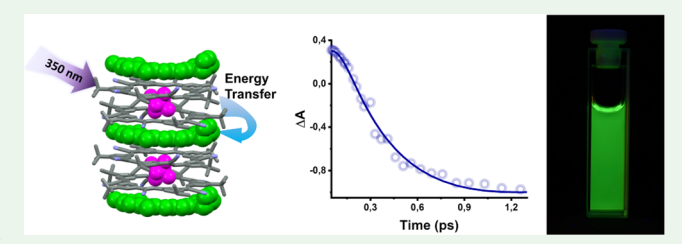
ACCESS

III Metrics & More

Article Recommendations

SI Supporting Information

ABSTRACT: Fluorescent nanoparticles based on organic dyes are promising materials for bioimaging applications. Recently, ultrabright fluorescent nanoparticles with orange emission were obtained by hierarchical coassembly of a cationic rhodamine dye with cyanostar anion-receptor to produce small-molecule ionic isolation lattices (SMILES). The cyanostar anion-complexes provides spatial and electronic isolation of the rhodamine dye prohibiting aggregation quenching. Cyanostar also constitutes a UV excitation antenna system to boost the brightness of the



rhodamine SMILES nanoparticles due to a large molar absorption coefficient in the UV region and efficient energy transfer to the dye. To further study the UV light harvesting process, we compared the rhodamine SMILES nanoparticles to green emissive cyanine-based SMILES nanoparticles, different in spectral overlap between cyanostar and the dye molecules. The energy transfer efficiency is increased from 80% in rhodamine SMILES to 100% in cyanine SMILES NPs due to increased spectral overlap. The energy transfer process was studied in detail by using femtosecond (fs) transient absorption (TA) spectroscopy, yielding energy transfer time-constants of around 0.4 and 1.3 ps for the cyanine- and rhodamine-based SMILES NPs, respectively. This result correlates well with the spectral overlap integrals and accounts for increased energy transfer and UV light harvesting efficiency. This insight into the UV light energy harvesting processes in the supramolecular SMILES materials will aid future design of ultrabright functional nanomaterials.

KEYWORDS: SMILES, fluorescent nanoparticles, aggregation-caused quenching, fluorescent dyes, energy transfer, light harvesting, antenna effect

■ INTRODUCTION

Organic dyes provide an attractive and promising starting point for constructing fluorescent nanoparticles (NPs) with the potential for applications in bioimaging. 1,2 Organic dyes have highly tunable optical properties that derive from atomic editing of their covalent structure, and they are free from toxic elements often present in inorganic NPs. 1-5 However, it is fundamentally challenging to transfer the attractive optical properties of organic dyes from the solution state to the highdensity solids of NP materials. One of the main obstacles is aggregation-caused quenching (ACQ) that is attributed to a collection of phenomena. First, the close packing of traditional organic dyes in crystals or aggregated states leads to strong electronic coupling between the chromophores, inducing spectral shifts and new electronic transitions, often with low radiative yields as a consequence. 6-10 Second, even when a specific structure has a high radiative yield, the photongenerated excitons easily migrate between the densely packed dyes to nonemissive defects, e.g., on the surface of the NPs, resulting in significant quenching of fluorescence. 11-14 Different strategies have been proposed to reduce aggregation caused quenching and improve the brightness of organic dyeloaded fluorescent NPs. The most common of these includes: covalent introduction of bulky side groups onto organic dyes and conjugated polymers, pairing cationic dyes with large hydrophobic counterions, supramolecular encapsulation, and dilution in matrices, e.g., polymers, silica, and ionic liquids. $^{2,15-22}_{}$ Another approach is the use of special dye types that are less susceptible to quenching, this includes the so-called, aggregation-induced emission dyes. $^{23-26}_{}$

Recently, we created small-molecule ionic isolation lattices (SMILES)²⁷ that solve the problem of strong coupling between dyes and thus help diminishes aggregation-caused quenching. These materials simultaneously organize cationic dyes into densely packed structures while keeping them well separated by large disc-shaped anion complexes formed between added anion receptors (cyanostar, CS) and the

Special Issue: Professor Sir Fraser Stoddart's 80th Birthday Forum

Received: May 2, 2022 Accepted: June 26, 2022 Published: July 12, 2022





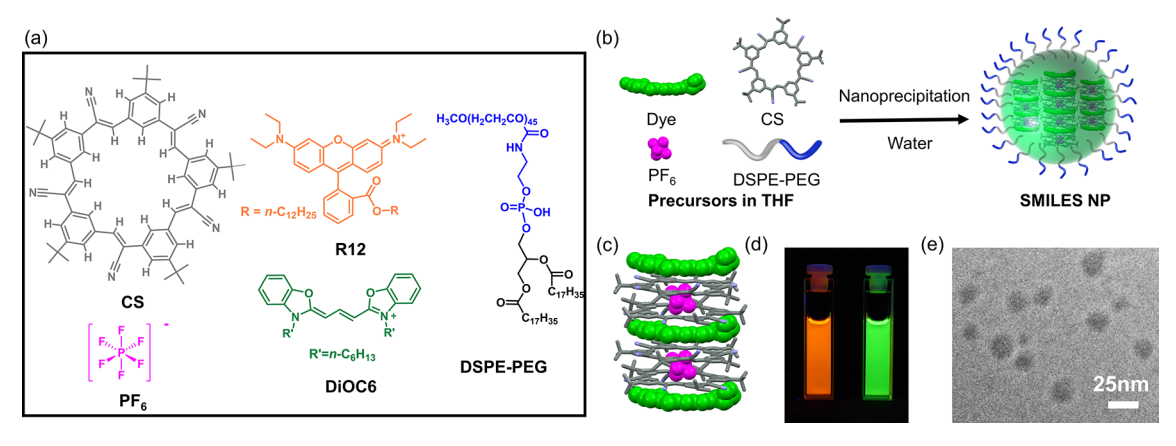


Figure 1. (a) Molecular structures of cationic dyes R12 and DiOC6, counteranion (PF₆⁻), anion binding cyanostar (CS), and amphiphilic surface capping agent DSPE-PEG. (b) Schematic illustration of the nanoprecipitation for preparing DSPE-PEG-capped SMILES NPs. (c) Charge-by-charge packing motif in SMILES materials. (d) Photograph of R12 (orange) and DiOC6 (green) SMILES NP emission in water under UV light. (e) Cryo-TEM image of R12 SMILES NPs capped with 66 wt % DSPE-PEG.

anions accompanying the fluorescent dyes (Figure 1). This new strategy for making fluorescent solids was found to be generally applicable to the most important cationic dye classes (e.g., rhodamines, oxazines, styryls, cyanines, and trianguleniums), which all crystallized in strikingly similar stacked, charge-alternating structures (Figure 1C) with highly improved emission brightness.²⁷ We recently translated the SMILES concept from bulk solids to solids on the nanometer length scale. We made biocompatible fluorescent NPs with orangecolored emission using a rhodamine dye (R12), cyanostar, and an amphiphilic surface capping agent (Figure 1).²⁸ These SMILES NPs showed high brightness, high photostability, high biocompatibility, and broad scope for introducing advanced optical properties for bioimaging. We found that the cyanostar molecules play multiple functions in these SMILES NPs.^{27,28} First, they are preventing aggregation-caused quenching by acting as a structure directing spacer between the cationic dyes. Second, the overall fluorescence quantum yield of the SMILES NPs can be increased by excess cyanostar molecules which passivate defect sites in the SMILES NPs.²⁸ Third, the cyanostar molecules can boost the brightness of SMILES NPs by taking advantage of their large molar absorption coefficient in the UV region and constituting a UV light harvesting system.²⁸ Followed by UV excitation of the cyanostar molecules, the energy can efficiently funnel to the fluoresencent dyes in the SMILES lattice. This feature of the lattice is unique when compared to other molecular spacers, e.g., large hydrophobic counterions¹³ and matrices like polymers,¹⁹ silica,²² and ionic liquids²¹ applied in dye-loaded NPs. This feature lends additional brightness and functionality to the SMILES NPs. The discovery of the UV light harvesting effect in SMILES NPs lays the groundwork to explore the origin of the boosted brightness of SMILES NPs in the UV region in more detail.

In this work, we study the UV light energy harvesting feature of the cyanostar molecules and the SMILES lattice to elucidate which parameters control the energy transfer process and how to modulate the UV light harvesting. We developed two types of SMILES NPs capable of displaying orange and green emission and thus with different excited state energies to interact with and receive energy from the UV excited cyanostar molecules. We selected two different dyes to form SMILES NPs (Figure 1, R12 dye for orange emission; DiOC6 dye for

green emission). We observe that the energy-transfer efficiency is increased from 83% in the NPs with orange-emission to 100% in the SMILES NPs with green emission. The energy transfer process was studied by using femtosecond (fs) transient absorption (TA) spectroscopy. Based on the fs-TA results, we identified a fast energy transfer process with a time-constant of 400 fs in the green SMILES NPs, which accounts for its 100% energy transfer efficiency. Furthermore, we find that the rates and efficiencies of energy transfer are correlated with the spectral overlap integrals, as predicted by theory. This offers a perfect framework to engineer the energy flow in SMILES nanomaterials for UV light harvesting.

■ RESULTS AND DISCUSSION

We synthesized SMILES NPs with orange and green fluorescence following our previously reported nanoprecipitation procedure.²⁸ Briefly, a precursor solution was prepared by dissolving all components needed to form SMILES NPs in tetrahydrofuran (THF), namely the cationic dye (R12 or DiOC6) as PF₆⁻ salt, the cyanostar anion receptor (2.5 mol equiv), and 66 wt % amphiphilic surface capping agent (1,2distearoyl-sn-glycero-3-phosphoethanolamine-poly(ethylene glycol-2000) (DSPE-PEG)). 2.5 mol equiv of cyanostar was used to prepare SMILES NPs because our previous study has shown that the brightness per volume of the R12-SMILES NPs reaches a maximum with 2.5 mol equiv of cyanostar.²⁸ The SMILES NPs were formed by injecting this precursor solution (0.5 mL) into a large excess of water (10 mL) under sonication for 1 min. For the first time, we developed the green emission SMILES NPs simply by replacing the R12 dye with DiOC6 dye in the precursor solution. The DiOC6 SMILES NPs show emission peak at around 515 nm (Figure 2). The hydrodynamic size of the new DiOC6-based green SMILES NPs was found to be 14 ± 2 nm, based on dynamic light scattering measurements (Figure S1). The hydrodynamic size of DiOC6based SMILES NPs is slightly smaller than that of the orange R12-based SMILES NP $(16 \pm 2)^{28}$ Cryo-TEM images of DiOC6 SMILES NPs show comparable size to DLS as previously also confirmed for R12 SMILES NPs (Figures S3 and 1e). The similarity in size between R12 and DiOC6 SMILES NPs indicates that the exact structure of the dye has little influence on the size of the NPs and is consistent with the high structural similarity between SMILES crystal structures

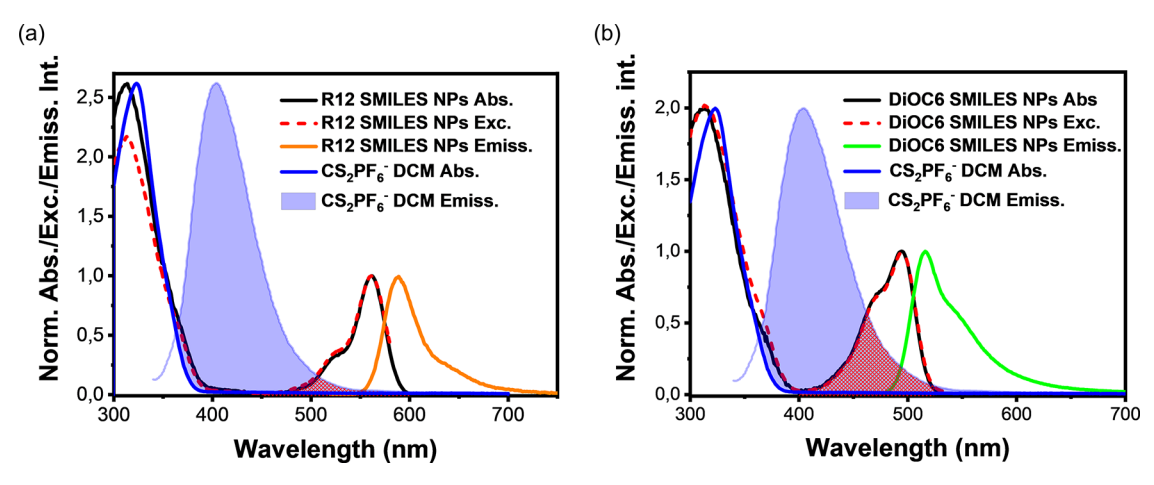


Figure 2. Normalized absorption, emission, and excitation spectra of (a) R12 (510 nm excitation and 650 nm emission detection) and (b) DiOC6 (470 nm excitation and 550 nm emission detection) based SMILES NPs. The absorption and emission spectra of the cyanostar anion complex $(CS_2PF_6^-)$ recorded in dichloromethane solution is shown as blue and shaded blue, respectively. The red area indicates relative spectral overlap between the emission of the $CS_2PF_6^-$ complex and the dye's absorption spectra (normalizations applied here do not correspond to the quantitative estimates of the overlap integrals J).

composed of different classes of cationic dyes.²⁷ On the basis of the overall composition of the SMILES NPs, we deduce that the average 15 nm NPs contains ~200 dyes.²⁸ Aqueous solutions of both NPs were found to be stable over weeks of storage at ambient conditions (Figure S2). The fluorescence quantum yields were determined to be 12.8% for R12 SMILES NPs and 7.2% for DiOC6 SMILES NPs. The quantum yields are lower than found for the dyes in SMILES crystals,²⁷ and we attribute this to a higher number of trap states in the small NP structure. This agrees with the shorter and multiexponential fluorescence lifetimes of the SMILES NPs, 1.11 and 0.52 ns for R12 and DiOC6, respectively (Table S1).

The absorption and emission spectra of the two SMILES NPs (Figure 2) resemble closely the spectra of dilute solutions (Figure S4), indicating successful generation of the SMILES lattices that prohibit close dye-dye contacts and strong electronic coupling. NPs without cyanostar display aggregated spectra and strongly reduced emission yields as previously reported for R12²⁸ and shown in Figure S5 for DiOC6. In addition to the $S_0 \rightarrow S_1$ absorption bands from the R12 and DiOC6 dyes at 561 and 495 nm, respectively, both NPs display an intense UV absorption band peaking at 313 nm ($\varepsilon \approx 2.5 \times$ 10⁵ M⁻¹ cm⁻¹)²⁹ assigned to the cyanostar anion complex (CS₂PF₆⁻). Solution absorption and emission spectra of the complex is shown for comparison. There is a clear spectral overlap between the fluorescence of the cyanostar anion complex and the absorption of the dye molecules (R12 or DiOC6, Figure 2, red shaded areas). The spectral overlap and the short distance (<1 nm) between cyanostar and dye molecules in the lattice offer ideal conditions for cyanostar-todye energy transfer. In the SMILES lattices each cyanostar anion complex is in van der Waals contact with two potential acceptor dyes as sketched in Figure 1C.²⁷ The efficiency of the energy transfer process can be estimated from the excitation spectrum of the acceptor (dye molecules: R12 or DiOC6). At a specific wavelength, the excitation intensity (I) of the acceptor can be calculated as $I = A_a + \phi_{ET}A_d$, in which A_a and A_d represent the absorbance of the energy acceptor and donor (cyanostar). Without energy transfer, the excitation spectrum of the acceptor is the same as the absorption spectrum of the acceptor. For $\phi_{\rm ET}$ = 100%, the excitation spectrum matches the

sum of the absorption spectrum of the acceptor and donor.³⁰ In the current work, the acceptors do not show any absorbance at the donor (cyanostar) band at 320 nm. Hence, the efficiency can be estimated by the intensity ratio between the NP excitation and absorption spectra³⁰ for the cyanostar band at 320 nm, when the two spectra are normalized to the $S_0 \rightarrow S_1$ absorption bands of the dye components, as in Figure 2. The estimated energy transfer is 83% and 100% for R12 and DiOC6 SMILES NPs, respectively. To ensure that these numbers are as accurate as possible, the excitation spectra were corrected for variations in excitation intensity and detector sensitivity of the setup across the relevant spectral range using several dye solutions (see the Supporting Information for details). This process allowed us to correct the original reported energy transfer efficiency of the R12 SMILES NPs from $\approx 50\%^{28}$ to 83%. These high energy transfer efficiencies and the large absorption cross section of cyanostar result in a 2-fold increase in brightness of both R12 and DiOC6 SMILES NPs when using 320 nm excitation compared to direct excitations of the dyes in the visible range, as reflected directly in the value of the normalized excitation spectral at 320 nm (Figure 2). Emission spectra of the SMILES NPs using 320 nm excitation showed very low residual cyanostar emission, Figure S6. This very low intensity of remaining cyanostar emission corresponds well with the high energy transfer efficiency in both R12 or DiOC6 SMILES NPs.

To gain further insight into the energy transfer between cyanostar and the dye molecules (R12 or DiOC6) in the two types of SMILES NPs, we carried out fs-TA spectroscopy. In the fs-TA experiment, we selectively excited the SMILES NPs with 350 nm pump laser (details in the Supporting Information). At 350 nm, the absorption of cyanostar is at least 15 times higher than that of both dye molecules (Figure S4). As a result, the cyanostar molecules are selectively excited. In this way, we can study the energy transfer process from photoexcited cyanostar to the dye molecules. Two obvious features appear in the pseudocolor fs-TA spectrogram (Figure 3) of R12 SMILES NPs: we see a negative ground state bleach (GSB, blue) signal located around 560 nm and a positive excited state absorption (ESA, red) signal with a broad spectral feature in the 420–800 nm range. The broad ESA signal is

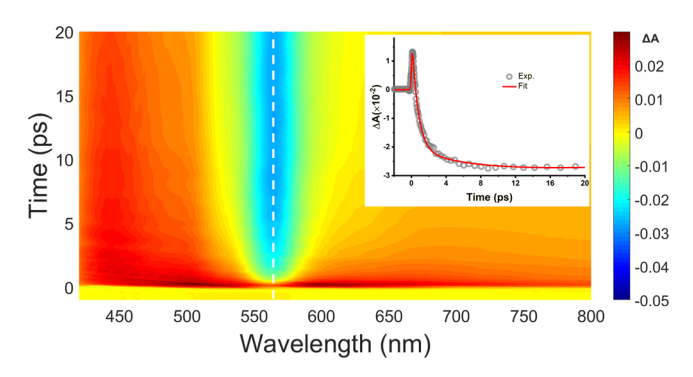


Figure 3. Pseudocolor representation TA spectra of R12-based SMILES NPs with 350 nm excitation (insert: signal and fit at 560 nm).

mainly assigned to the cyanostar molecules based on the observation of a broad ESA signal for the cyanostar alone when excited with a 350 nm pump (Figure S7). Upon energy transfer from the photoexcited cyanostar to the dye molecules, the positive ESA signal (formed right after excitation) decays and it is replaced by a strong negative GSB signal in the region of the dye's main absorption band, as clearly seen in the TA signal at 560 nm (Figure 3, inset).

The two types of SMILES NPs with different dyes (R12 or DiOC6) show analogous GSB and ESA features although the GSB position and the time constants vary (Figures 3 and S8). The growth of the GSB signal indicates the formation of the excited dyes and is thus the result of energy transfer from the initially photoexcited cyanostar. The GSB builds up with different rates in the two types of SMILES NPs (Figures 3 and S8). The GSB of DiOC6-based SMILES NPs builds up much faster than R12-based SMILES NPs. This observation indicates that energy transfer happens at significantly different rates in the two types of NPs.

We determined the time-constant of the energy transfer process using a global fit to the TA spectra involving a sum of exponentials with global time-constants as variables (details in the Supporting Information). In the global fitting, a sequential model is used to obtain the excited state lifetime ($\tau_{\rm CS^*}$) of the cyanostar in R12 SMLES NPs and DiOC6 SMILES NPs. The energy transfer time-constant ($\tau_{\rm ET}$) can be calculated based on $\phi_{\rm ET} = k_{\rm ET}/k_{\rm CS^*}$, in which $k_{\rm ET} = 1/\tau_{\rm ET}$, $k_{\rm CS^*} = 1/\tau_{\rm CS^*}$. The calculated results are as listed in Table 1. The outcome of fitting using the sequential model results in evolution-associated spectra. For each SMILES NP, two evolution-associated spectra were needed to describe the dynamics with 350 nm laser excitation (Figure 4a,b).

The number of evolution-associated spectra corresponds to the number of species involved in the relaxation of the SMILES NPs after photoexcitation. The excitation of cyanostar can be represented as CS*. This state transfers its energy to the dye molecule (R12 or DiOC6), forming excited dye molecules (R12* or DiOC6*), and returns to the ground state cyanostar

(CS) within the SMILES NPs. The excited dye molecules are long-lived states that decay in a few nanoseconds by fluorescence and competing nonradiative internal conversion (Figure S9 and Table S1). In general, the spectral shape of CS* matches well with the TA spectra of CS in THF (Figure S7), except for a distortion appearing at the position where dye molecules show the strongest GSB signal: the $S_0 \rightarrow S_1$ absorption bands from the R12 and DiOC6 dyes at 561 and 495 nm, respectively. Such a distortion might be caused by two reasons. First, the spectral shape of CS* is evolving with time, specifically showing a shift in the peak position (Figure S7).³² Second a small amount of dye molecules was excited by the 350 nm pump pulse. Given that the absorption coefficient of the dye molecules at 350 nm is about 20 times lower than cyanostar, such a spectral distortion has a negligible impact on the retrieval of the time-constant of the energy transfer from CS* to dye molecules.

The time-constant of the energy transfer (Table 1) from CS* to dye molecule is 1.6 and 0.4 ps in R12 SMILES NPs and DiOC6 SMILES NPs, respectively. The energy transfer process in DiOC6 SMILES NPs is thus much faster than that in R12 SMILES NPs. This rate difference agrees with the higher energy transfer efficiency in DiOC6 SMILES NPs, Φ_{ET} = 100% relative to Φ_{ET} = 80% for R12. While, the observed time-constants in the picoseconds range explains the high transfer efficiency, these rates are still an order of magnitude lower than the very fast transfer rates that has been reported for homo-FRET between individual rhodamine dyes in dye-loaded nanoparticles with high dye concentrations.³³

In the SMILES structure, the cyanostar molecules are present in the form of anion complexes (CS₂PF₆⁻) and in proximal cofacial contact with the two nearest neighbor dyes, above and below in the alternating stack (Figure 1C), at distances close to van der Waals contact. Under these conditions both exchange (Dexter) and resonant (Förster) energy transfer mechanisms are highly efficient and can be expected to contribute. The classical Förster equation cannot be expected to provide quantitative predictions as a result of the breakdown of the point dipole approximation at such short distances. 11,34 However, the energy transfer rate is still expected to be proportional to the spectra overlap integral (*J*) between donor (CS*) emission and acceptor (dye) absorption for both Förster and Dexter transfer. The spectral overlap in DiOC6 is significantly larger than that in R12 (Figure 2 and Table S2). This difference accounts for the increased energy-transfer efficiency and speed in the DiOC6 SMILES NPs, even though the transfer to R12 is more exergonic. The spectral overlap integrals applied in Förster $(I_{\rm F})$ and Dexter (J_D) theory differ from each other by inclusion of the absorption probability ($\varepsilon_{\rm dye}$) of the acceptor in $J_{\rm F}$. Calculation of J values (see the Supporting Information) for energy transfer from CS₂PF₆⁻ to DiOC6 and R12 predicts $J_{\rm F}({\rm DiOC6})$ to be four times greater than $J_{\rm F}({\rm R}12)$, while this ratio is three when calculating J_D (Table S2). The J_F ratio

Table 1. Summary of the Energy Transfer Parameters, Fluorescence Quantum Yield (FQY), Brightness of SMILES NPs with Different Dye Molecules (R12 or DiOC6)

SMILES NP dye	$ au_{\mathrm{CS}^*}$ (ps)	$ au_{\mathrm{ET}}\ (\mathrm{ps})$	$\phi_{ ext{ET}}$	FQY ^a (directly excited)	brightness (directly excited) ^b	brightness ($\lambda_{ex} = 320 \text{ nm}$)
R12	1.3	1.6	80%	12.8%	12400	21000
DiOC6	0.4	0.4	100%	7.2%	10300	20600

^aFQY: fluorescence quantum yield. ^bBrightness per formula unit, with direct excitation of the dye molecules' absorption peak with lowest energy.

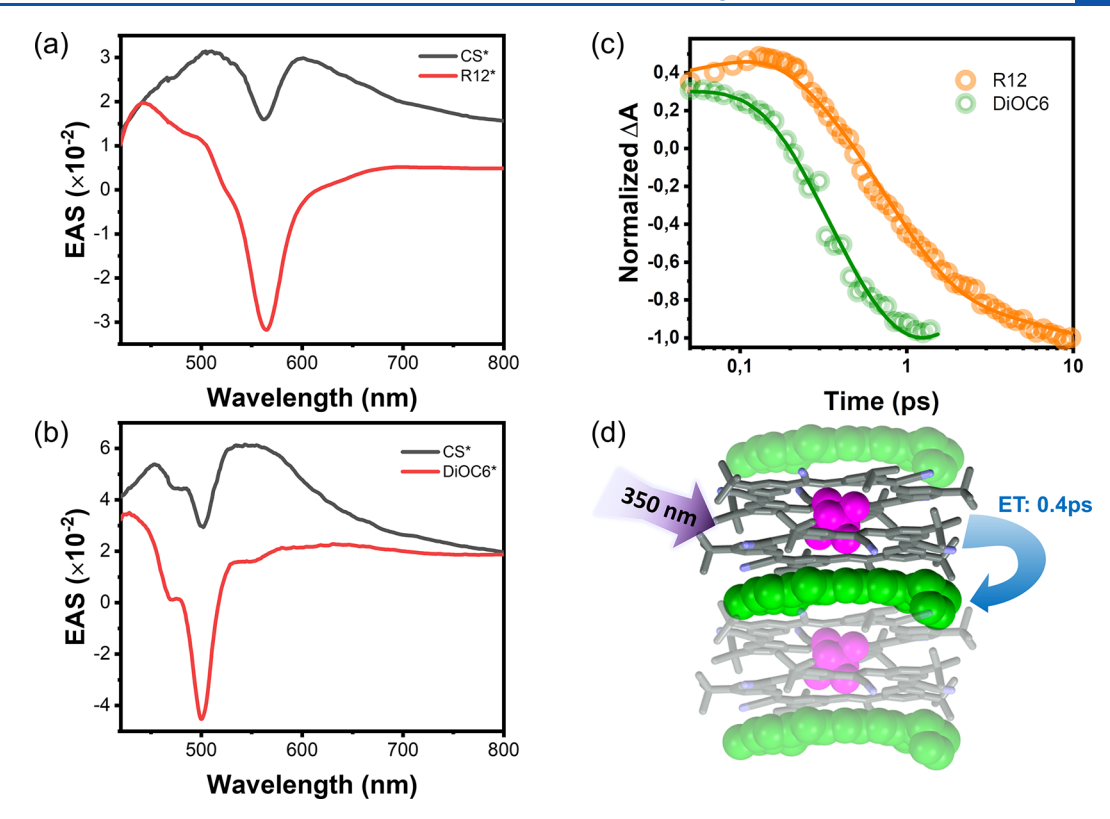


Figure 4. (a,b) Evolution-associated spectra of R12 SMILES NPs (a) and DiOC6 SMILES NPs (b); (c) normalized ground state bleach signal of R12 SMILES NPs (orange color) and DiOC6 SMILES NPs (green color); and (d) energy transfer process from CS* to dye molecules (R12 or DiOC6).

agrees very well with the difference in transfer rates reflected in the time constants of 0.4 ps for DiOC6 and 1.6 ps for R12 (factor of 4), this could indicate that the energy transfer mechanism is a dominantly Förster-like transfer where the magnitude of the donor and acceptor transition dipoles is important. However, the relatively small difference between $J_{\rm F}$ and $J_{\rm D}$ ratios for CS* to dye transfer for these two dyes does not allow us to exclude Dexter transfer.

CONCLUSION

In conclusion, we provided the first detailed study of the energy transfer from cyanostar to dye molecules in SMILES NPs and demonstrated how this process enhanced the brightness of SMILES NPs by harvesting the UV light. Our preparation of SMILES NPs using cyanine dye DiOC6 allowed us to assign the enhanced brightness seen with cyanostar excitation to efficient energy transfer processes. The new green emissive SMILES NPs have a size of 14 ± 2 nm, similar to SMILES NPs obtained with the rhodamine dye R12, and both dyes retain their spectral properties from dilute solutions, emphasizing the robustness of the SMILES principle and the nanoprecipitation-based synthesis of SMILES NPs. For both SMILES NPs, the emission brightness is enhanced by approximately 100% when exciting the cyanostar component of the SMILES lattice with UV light harvesting. The efficiency of this UV light energy harvesting (UV sensitization) relies on an ultrafast energy transfer at the subpicosecond time scale, which scales with the spectral overlap integral between cyanostar as energy donor and the acceptor dye embedded in the SMILES lattice. The detailed understanding of the energy transfer process and how it is linked to the photo

physical properties of the applied dyes offers us a strategy on engineering the energy flow in SMILES NPs.

ASSOCIATED CONTENT

Supporting Information

The Supporting Information is available free of charge at https://pubs.acs.org/doi/10.1021/acsanm.2c01899.

Material and chemicals, SMILES NPs preparation, dynamic light scattering (DLS) measurements, spectroscopic characterization, cryo-TEM, correction of excitation spectra, fs-TA spectroscopy, global analysis of fs-TA spectra, fluorescence decay, molar absorption coefficient of DiOC6 in SMILES NPs, and calculation of spectra overlap integrals (PDF)

AUTHOR INFORMATION

Corresponding Authors

Amar H. Flood — Department of Chemistry, Indiana University, Bloomington, Indiana 47405, United States; orcid.org/0000-0002-2764-9155; Email: aflood@indiana.edu

Bo W. Laursen – Nano-Science Center & Department of Chemistry, University of Copenhagen, 2100 København Ø, Denmark; orcid.org/0000-0002-1120-3191; Email: bwl@nano.ku.dk

Authors

Junsheng Chen – Nano-Science Center & Department of Chemistry, University of Copenhagen, 2100 København Ø, Denmark; orcid.org/0000-0002-2934-8030

- Stine G. Stenspil Nano-Science Center & Department of Chemistry, University of Copenhagen, 2100 København Ø, Denmark; ⊚ orcid.org/0000-0002-0252-6829
- Spyridon Kaziannis ELI Beamlines, Institute of Physics, Czech Academy of Sciences, 252 41 Dolní Břežany, Czech Republic; Department of Physics, University of Ioannina, Ioannina, GR 54110, Greece
- Laura Kacenauskaite Nano-Science Center & Department of Chemistry, University of Copenhagen, 2100 København Ø, Denmark
- Nils Lenngren ELI Beamlines, Institute of Physics, Czech Academy of Sciences, 252 41 Dolní Břežany, Czech Republic; orcid.org/0000-0001-7563-9843
- Miroslav Kloz ELI Beamlines, Institute of Physics, Czech Academy of Sciences, 252 41 Dolní Břežany, Czech Republic

Complete contact information is available at: https://pubs.acs.org/10.1021/acsanm.2c01899

Author Contributions

¹J.C. and S.G.S. contributed equally.

Notes

The authors declare no competing financial interest.

ACKNOWLEDGMENTS

This work was supported by the Lundbeck Foundation (Grant R303-2018-3237), Danish Council of Independent Research (DFF-0136-00122B), and the Czech Science Foundation (21-09692M; M.K.). A.H.F. thanks the National Science Foundation (DMR-2118423) for support.

DEDICATION

The work is dedicated to Fraser Stoddart on the event of his 80th birthday and recognizes the stimulating lab environment he created at UCLA. It allowed Flood and Laursen to meet and, many years later, helped them forge a new collaboration on the fluorescent materials outlined in this present work.

REFERENCES

- (1) Middha, E.; Liu, B. Nanoparticles of Organic Electronic Materials for Biomedical Applications. ACS Nano 2020, 14 (8), 9228–9242.
- (2) Reisch, A.; Klymchenko, A. S. Fluorescent Polymer Nanoparticles Based on Dyes: Seeking Brighter Tools for Bioimaging. *Small* **2016**, *12* (15), 1968–1992.
- (3) Klymchenko, A. S.; Liu, F.; Collot, M.; Anton, N. Dye-Loaded Nanoemulsions: Biomimetic Fluorescent Nanocarriers for Bioimaging and Nanomedicine. *Adv. Healthc Mater.* **2021**, *10* (1), No. 2001289.
- (4) Fang, F.; Li, M.; Zhang, J.; Lee, C.-S. Different Strategies for Organic Nanoparticle Preparation in Biomedicine. *ACS Materials Letters* **2020**, 2 (5), 531–549.
- (5) Wani, W. A.; Shahid, M.; Hussain, A.; AlAjmi, M. F. Fluorescent Organic Nanoparticle; Springer, 2018.
- (6) Cornil, J.; Beljonne, D.; Calbert, J. P.; Bredas, J. L. Interchain Interactions in Organic Pi-Conjugated Materials: Impact on Electronic Structure, Optical Response, and Charge Transport. *Adv. Mater.* **2001**, *13* (14), 1053–1067.
- (7) Kasha, M.; Rawls, H. R.; Ashraf El-Bayoumi, M. The exciton model in molecular spectroscopy. *Pure Appl. Chem.* **1965**, *11*, 371–392.
- (8) Birks, J. B. *Photophysics of Aromatic Molecules*; Wiley-Interscience: London, 1970.
- (9) Huang, Y. J.; Xing, J.; Gong, Q. Y.; Chen, L. C.; Liu, G. F.; Yao, C. J.; Wang, Z. R.; Zhang, H. L.; Chen, Z.; Zhang, Q. C. Reducing

- Aggregation Caused Quenching Effect through Co-Assembly of PAH Chromophores and Molecular Barriers. Nat. Commun. 2019, 10, 169.
- (10) Karki, K. J.; Chen, J.; Sakurai, A.; Shi, Q.; Gardiner, A. T.; Kuhn, O.; Cogdell, R. J.; Pullerits, T. Before Forster. Initial excitation in photosynthetic light harvesting. *Chem. Sci.* **2019**, *10* (34), 7923–7928.
- (11) Gierschner, J.; Shi, J.; Milián-Medina, B.; Roca-Sanjuán, D.; Varghese, S.; Park, S. Luminescence in Crystalline Organic Materials: From Molecules to Molecular Solids. *Adv. Opt Mater.* **2021**, 9 (13), 2002251.
- (12) Genovese, D.; Rampazzo, E.; Bonacchi, S.; Montalti, M.; Zaccheroni, N.; Prodi, L. Energy transfer processes in dye-doped nanostructures yield cooperative and versatile fluorescent probes. *Nanoscale* **2014**, *6* (6), 3022–3036.
- (13) Reisch, A.; Didier, P.; Richert, L.; Oncul, S.; Arntz, Y.; Mely, Y.; Klymchenko, A. S. Collective Fluorescence Switching of Counterion-Assembled Dyes in Polymer Nanoparticles. *Nat. Commun.* **2014**, *5*, 4089.
- (14) Chen, J.; Zidek, K.; Abdellah, M.; Al-Marri, M. J.; Zheng, K. B.; Pullerits, T. Surface plasmon inhibited photo-luminescence activation in CdSe/ZnS core-shell quantum dots. *J. Phys.: Condens. Matter* **2016**, 28, 254001.
- (15) Wang, Y.; Wu, H.; Hu, W.; Stoddart, J. F. Color-Tunable Supramolecular Luminescent Materials. *Adv. Mater.* **2022**, *34* (22), No. 2105405.
- (16) Stolte, M.; Schembri, T.; Süß, J.; Schmidt, D.; Krause, A.-M.; Vysotsky, M. O.; Würthner, F. 1-Mono- and 1,7-Disubstituted Perylene Bisimide Dyes with Voluminous Groups at Bay Positions: In Search for Highly Effective Solid-State Fluorescence Materials. *Chem. Mater.* 2020, 32 (14), 6222–6236.
- (17) Yang, Y.; Sun, C.; Wang, S.; Yan, K.; Zhao, M.; Wu, B.; Zhang, F. Counterion-Paired Bright Heptamethine Fluorophores with NIR-II Excitation and Emission Enable Multiplexed Biomedical Imaging. *Angew. Chem., Int. Ed. Engl.* **2022**, *61* (24), No. e202117436.
- (18) Yang, J.-S.; Swager, T. M. Porous Shape Persistent Fluorescent Polymer Films: An Approach to TNT Sensory Materials. *J. Am. Chem. Soc.* 1998, 120 (21), 5321–5322.
- (19) Grazon, C.; Rieger, J.; Meallet-Renault, R.; Charleux, B.; Clavier, G. Ultrabright Fluorescent Polymeric Nanoparticles Made from a New Family of BODIPY Monomers. *Macromolecules* **2013**, 46 (13), 5167–5176.
- (20) Tian, Z.; Shaller, A. D.; Li, A. D. Twisted Perylene Dyes Enable Highly Fluorescent and Photostable Nanoparticles. *Chem. Commun.* **2009**, 2 (2), 180–182.
- (21) Cui, K.; Lu, X. M.; Cui, W.; Wu, J.; Chen, X. M.; Lu, Q. H. Fluorescent Nanoparticles Assembled from a Poly(Ionic Liquid) for Selective Sensing of Copper Ions. *Chem. Commun.* **2011**, 47 (3), 920–922.
- (22) Chen, W.; Cheng, C. A.; Cosco, E. D.; Ramakrishnan, S.; Lingg, J. G. P.; Bruns, O. T.; Zink, J. I.; Sletten, E. M. Shortwave Infrared Imaging with J-Aggregates Stabilized in Hollow Mesoporous Silica Nanoparticles. *J. Am. Chem. Soc.* **2019**, *141* (32), 12475–12480.
- (23) Würthner, F. Aggregation-Induced Emission (AIE): A Historical Perspective. *Angew. Chem., Int. Ed. Engl.* **2020**, 59 (34), 14192–14196.
- (24) Li, K.; Liu, B. Polymer-Encapsulated Organic Nanoparticles for Fluorescence and Photoacoustic Imaging. *Chem. Soc. Rev.* **2014**, 43 (18), 6570–6597.
- (25) Cai, X. L.; Liu, B. Aggregation-Induced Emission: Recent Advances in Materials and Biomedical Applications. *Angew. Chem., Int. Ed. Engl.* **2020**, *59* (25), 9868–9886.
- (26) Qian, J.; Tang, B. Z. AIE Luminogens for Bioimaging and Theranostics: from Organelles to Animals. *Chem.* **2017**, 3 (1), 56–91. (27) Benson, C. R.; Kacenauskaite, L.; VanDenburgh, K. L.; Zhao, W.; Qiao, B.; Sadhukhan, T.; Pink, M.; Chen, J. S.; Borgi, S.; Chen, C. H.; Davis, B. J.; Simon, Y. C.; Raghavachari, K.; Laursen, B. W.; Flood, A. H. Plug-and-Play Optical Materials from Fluorescent Dyes and Macrocycles. *Chem.* **2020**, 6 (8), 1978–1997.

- (28) Chen, J.; Fateminia, S. M. A.; Kacenauskaite, L.; Baerentsen, N.; Gronfeldt Stenspil, S.; Bredehoeft, J.; Martinez, K. L.; Flood, A. H.; Laursen, B. W. Ultrabright Fluorescent Organic Nanoparticles Based on Small-Molecule Ionic Isolation Lattices. Angew. Chem., Int, Ed. Engl. 2021, 60 (17), 9450-9458.
- (29) Lee, S.; Chen, C. H.; Flood, A. H. A Pentagonal Cyanostar Macrocycle with Cyanostilbene CH Donors Binds Anions and Forms Dialkylphosphate [3] Rotaxanes. Nat. Chem. 2013, 5 (8), 704-710.
- (30) Stryer, L.; Haugland, R. P. Energy Transfer a Spectroscopic Ruler. Proc. Natl. Acad. Sci. U. S. A. 1967, 58 (2), 719-726.
- (31) Chen, J. S.; Messing, M. E.; Zheng, K. B.; Pullerits, T. Cation-Dependent Hot Carrier Cooling in Halide Perovskite Nanocrystals. J. Am. Chem. Soc. 2019, 141 (8), 3532-3540.
- (32) Ruckebusch, C.; Sliwa, M.; Pernot, P.; de Juan, A.; Tauler, R. Comprehensive data analysis of femtosecond transient absorption spectra: A review. Journal of Photochemistry and Photobiology C: Photochemistry Reviews **2012**, 13 (1), 1–27.
- (33) Trofymchuk, K.; Reisch, A.; Didier, P.; Fras, F.; Gilliot, P.; Mely, Y.; Klymchenko, A. S. Giant light-harvesting nanoantenna for single-molecule detection in ambient light. Nat. Photonics 2017, 11 (10), 657-663.
- (34) Beljonne, D.; Curutchet, C.; Scholes, G. D.; Silbey, R. J. Beyond Förster Resonance Energy Transfer in Biological and Nanoscale Systems. J. Phys. Chem. B 2009, 113 (19), 6583-6599.

Recommended by ACS

Alkoxy-Substituted Quadrupolar Fluorescent Dyes

Yuanning Feng, J. Fraser Stoddart, et al. SEPTEMBER 09, 2022

JOURNAL OF THE AMERICAN CHEMICAL SOCIETY

READ **Z**

An Unlimited Color Palette from Perylene Derivative **Molecules Dispersed within Hybrids**

Yixuan Guo, Yongjun Feng, et al.

NOVEMBER 04, 2022

ACS APPLIED OPTICAL MATERIALS

READ **C**

"Awakening" of the S₂ Emission of Tricarbocyanine Dyes Stimulated by Interaction with Carbon Quantum Dots

Oleg P. Dimitriev, Aleksey B. Ryabitskii, et al.

JULY 14, 2022

THE JOURNAL OF PHYSICAL CHEMISTRY LETTERS

READ **C**

Repurposing Cyanine Photoinstability To Develop Near-Infrared Light-Activatable Nanogels for In Vivo Cargo **Delivery**

Rodrigo Tapia Hernandez, Jefferson Chan, et al.

SEPTEMBER 25, 2022

JOURNAL OF THE AMERICAN CHEMICAL SOCIETY

READ 2

Get More Suggestions >